ILASS 2008
Sep. 8-10, 2008, Como Lake, Italy

Paper ID ILASS08-7-4

PIEZO SPRAY DROP-SIZE MEASUREMENTS BY LASER DIFFRACTION TECHNIQUE IN PRESENCE OF MULTIPLE SCATTERING EFFECTS

Pisit Yongyingsakthavorn[1*], Jean Cousin[1], Christophe Dumouchel[1], Jerôme Helie[2]

[1]Pisit Yongyingsakthavorn, UMR 6614 - CORIA – Université et INSA de Rouen,
Avenue de l'Université, BP 12, 76801 Saint Etienne du Rouvray, France.
Tel.33 2-32-95-37-12 Fax. 33 2-32-91-04-85 email: yongying@coria.fr
[2]Continental, BP 1149, 1 av. Paul Ourliac, 31036 Toulouse cedex 1, France

ABSTRACT
This work investigates drop-size distribution measurements with a laser diffraction technique of sprays produced by a pintle type, outward-opening injector driven by a piezo-actuator at injection pressures up to 20 MPa. Considering the high injection pressures, multiple scattering effects are expected. The multiple scattering effects were first verified and it is found that these effects are negligible when the transmission is greater than 13%. This limit is far less than the one found by many works of the literature that reported a limit in transmission of the order of 40%. One of the reasons for this difference is believed to be due to the specific characteristic features of the present spray drop-size distributions. A procedure based on the correction of the light intensity collected by each diode has been developed to get rid of the undesirable multiple scattering effects. This procedure, which returns analytical correction factors as a function of the transmission, allows reliable drop-size distribution to be obtained for injection pressure up to 20 MPa. Among other results, it is found that the piezo injector produces bi-modal spray drop-size distributions at high injection pressure. Finally, these distributions are successfully modelized by the application of the MEF. According to the injection pressure, the mathematical drop-size distributions are functions of three or five parameters whose correlations with the injection pressure have been derived.

1 INTRODUCTION

There are a remarkable number of different gasoline engine concepts and technologies depending on the market specific requirements [1]. All researches are intended to reduce both fuel consumption and emission while maintaining a good drivability. To achieve these requirements, combustion performances have to be improved through the development of new combustion concepts and new injection systems.

Outward-opening Piezo injector is one technology developed for gasoline direct injection (GDI) engine where stratified combustion has to be achieved. With this strategy, a very accurate temporal and spatial control of both injection and ignition is needed. The spark must ignite the well-prepared mixture plume before diffusion effects dilute the air-fuel mixture beyond the lean limit for premixed-combustion. To obtain the optimal operation meeting emission standard, atomization process and stratified combustion are necessary to be studied [2, 3].

As understanding of atomization is vital to the further development of fuel injection systems, the optical diagnostic instrumentation and measurement approaches must be developed. There are many optical measurement techniques for drop sizing but the most commonly used are the Phase Doppler Particle Analysis (PDPA) and the laser diffraction technique. The laser diffraction technique reports spatial drop-size frequency while PDPA reports a temporal drop-size frequency. The laser diffraction is more practical to measure global drop-size distribution because it is much less time consuming. Although this technique does not provide local drop-size distribution like the PDPA, deconvolution technique now exists to recover this information [4-6].

Measurement becomes difficult when the spray is dense. PDPA measurements require a single particle in the probe volume. For dense sprays, this requirement is usually not satisfied. On the other hand, multiple light scattering can affect the dense spray drop-size distribution reported by the laser diffraction technique. Some works concluded that multiple scattering effects are negligible when transmission is higher than about 40% [7, 9].

Although, the Malvern Company has developed a patented multiple scattering correction [10] allowing spray measurements with transmission as low as 5% to be performed, it was found that this correction does not work well for all situations. For instance, Triballier et al. [9] concluded that when transmission is less than 40% the Spraytec correction option is not well adapted for large sprays.

To solve the multiple light scattering problem, empirical correcting factors were determined. Dodge [7] determined the correction factor for Sauter Mean Diameter (D_{32}) and Rosin-Rammler N parameter as a function of transmission and diameter. Gulder [11] also determined the correction factors for mean diameters D_{32} and D_{30} as a function of obscuration. Boyaval and Dumouchel [12] represented correction factors for the mean diameter (D_{43}) and the relative span factor (Δ_v) as the function of obscuration.

The laser diffraction technique is applied in this study to characterize Piezo spray because of the following reasons: (1) less time-consuming measurement, (2) high data acquisition rate, and (3) possibility to propose empirical multiple scattering correction for dense sprays.

This paper intends to address problems in drop size measurement by laser diffraction technique and to propose an experimental procedure to correct drop-size distribution in presence of multiple light scattering if the patented correction of the Spraytec is not adapted for Piezo spray.

2 EXPERIMENTAL SETUP AND PROCEDURE

2.1 Experimental Setup

Figure 1 shows the experimental setup. There are two pumps, low-pressure and high-pressure pumps, allowing injection pressures to be varied from 0.5 MPa up to 20 MPa. A pressure regulator controls the injection pressure and fluid temperature is maintained by a heat exchanger in a returning line (at 18±2 °C). Extraction system is used to collect the droplets out from testing area.

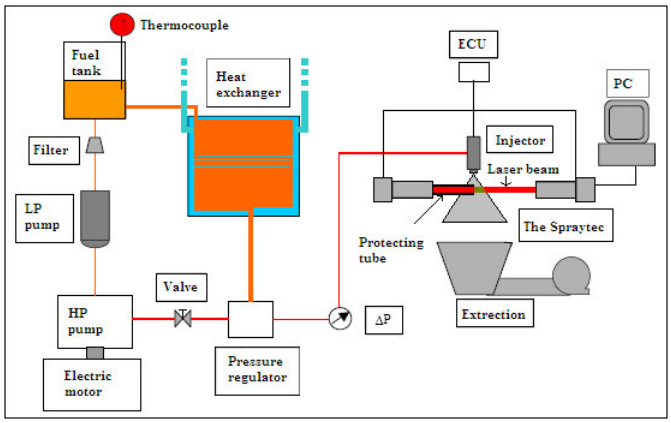

Fig. 1: The experimental setup.

Piezo injector with fast switching speed is tested. Thanks to relatively high injection pressure, small injection times are required to discharge the liquid. A piezoelectric actuator allows such times to be achieved. In addition, the actuation energy is tunable allowing the needle lift to be controlled. This kind of injector provides non-swirling conical sheets as shown in Fig. 2. The liquid sheet angle is 80°. For an injection pressure greater than about 5 MPa, the initial liquid sheet rearranges into streamwise ligaments contrary to pressure swirl atomizers. In such a situation, the ambient pressure does not influence the liquid cone angle and stratified mixtures can be realized [2, 3].

The drop-size distributions are measured by laser diffraction technique. The new equipment of Malvern Spraytec 2006, adapted to measure high-speed, transient and dense sprays, is employed. The wavelength of laser and its diameter are 632.8 nm and 10 mm, respectively. Measurement diameter range is 0.5–600 µm with the 300 mm lens. Measurements can be done at high acquisition rate up to 10 kHz and temporal evolution of drop-size distribution during a single injection event can be obtained. The minimum working distance is the distance between spray and the receiver where vignetting problem is not expected to happen. The Malvern Company increased this minimum working distance by using a larger detector.

Table 1: Properties of fluids

Liquid	ρ (kg/m^3)	ν (mm^2/s)	σ (mN/m)	P_v (kPa)	n
Gasoline	752	0.6	22.4	55-103	NA
Ex. D40	776	1.3	24.7	0.24	1.43

Exxsol D40 is used as working fluid because its vapor pressure is much lower than gasoline (see Table 1). This avoids the presence of vapor causing laser beam steering during the measurement. Its viscosity is higher than gasoline; while its surface tension and density are close to gasoline. The refractive index of Exxsol D40 is 1.43.

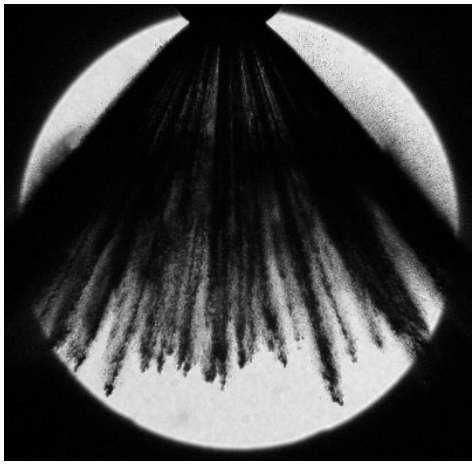

Fig. 2: Non-swirling conical sheet produced by Piezo injector (ΔP_i = 20 MPa).

2.2 Measurement Procedure

For each measurement, the laser beam center is positioned at 50 mm from the nozzle tip. The laser passes through the center of spray cross-section. Injection time (T_i) is 2 ms. For each condition, 25 injections with injection rate of 0.2 Hz were performed to determine representative spray evolution. Therefore, the representative drop-size distribution is averaged from 25 data. Averaging is carried out on scattered light intensity rather than on drop-size distribution. Then, the drop-size distribution is calculated from the averaged scattered light intensity distribution.

Figure 3 shows the temporal evolution of transmission for an injection pressure of 11 MPa. When the spray reaches the laser beam, transmission decreases sharply to a minimum value and then continuously increases. Contrary to other injection systems (see [12] for instance), the minimum transmission is not found constant during a time interval that would correspond to the body spray passage. This is a consequence of very short injection times. As expected this minimum transmission decreases with the injection pressure (see Fig. 4). As mentioned earlier, the multiple scattering effects are negligible when the transmission is greater than 40%. According to Fig. 4, this limit is reached for an injection pressure equal to 6 MPa. For greater injection pressure, the Malvern correction option should be selected. However, this correction is not valid when the transmission is lower than 5%, which limits the injection pressure to 13 MPa as shown in Fig. 4.

Preliminary tests revealed the presence beam steering and vignetting effects. Although Exxsol D40 has low vapor pressure, beam steering effect cannot be eluded. Beam steering is detected because high light intensity signals are found at the inner diodes. These signals lead to the presence of the unrealistic big drops (≈ 700–900 µm). The presence of fluid vapor, which causes variation of the refractive index in the measurement volume, is believed to be the consequence of internal flow cavitation effects. Furthermore, vignetting problem was also suspected. This problem is characterized by

small drop scattered light that escapes from the collection angle and is due to a high spray width where the measurements are performed.

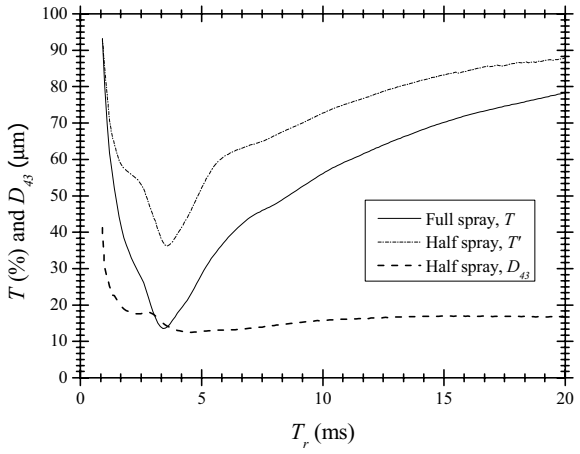

Fig. 3: Temporal evolutions of full and half spray transmissions and corresponding mean diameter D_{43} (ΔP_i = 11 MPa).

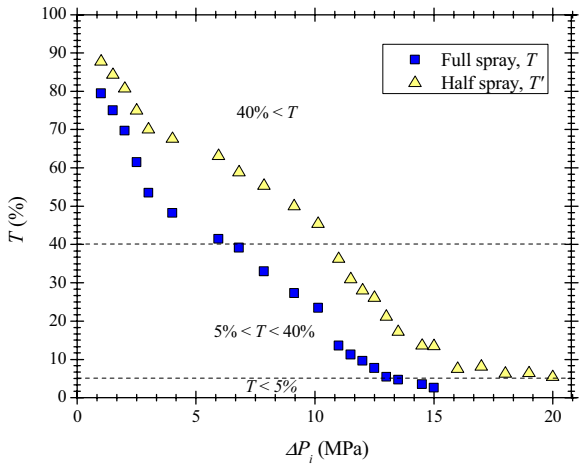

Fig. 4: Variation of the minimum transmission with the injection pressure.

To overcome these difficulties, measurements with a protecting tube as introduced by Boyaval and Dumouchel [12] is carried out. A protecting tube is employed to shield the laser beam so that only half of the spray interacts with the laser beam (see Fig. 1). Reducing the path length of the spray leads to an increase of transmission. Indeed, the light transmission can be written as:

$$T = e^{-\tau L_s} \tag{1}$$

where τ is the spray turbidity depending on the spray spatial density and on the scattering properties of the particles, and L_s is the length of the intersection zone between the spray and the laser beam. By using a protecting tube, the path length L_s is divided by 2 and the half-spray transmission becomes:

$$T' = \sqrt{T} \tag{2}$$

Figure 4 shows that with the protecting tube, multiple scattering effects are expected from an injection pressure of the order of 10 MPa, and measurements for injection pressures as high as 20 MPa become possible. In addition, it was noted that thanks to the protecting tube, the vignetting effects are reduced.

Half and full spray measurements are compared at the time where the transmission is minimum (see Fig. 3). It is believed that this minimum indicates similar aspect of the sprays. Figure 5 compares the transmissions obtained from full and half measurements. It is found that these transmissions agree well with Eq. (2). Furthermore, the axisymmetry of the drop-size distribution was checked by performing measurements with and without the tube at an injection pressure low enough (6 MPa) to guaranty the absence of multiple scattering effects when full spray measurement is performed. These measurements were conducted along several diameters of the spray by rotating the injector. In each situation, the full and half spray drop-size distributions were found to be the same as shown in Fig. 6. Therefore, the protecting has a negligible influence on the spray and the drop-size distribution is axisymmetric enough to consider that a half spray drop-size distribution is representative of the whole spray distribution.

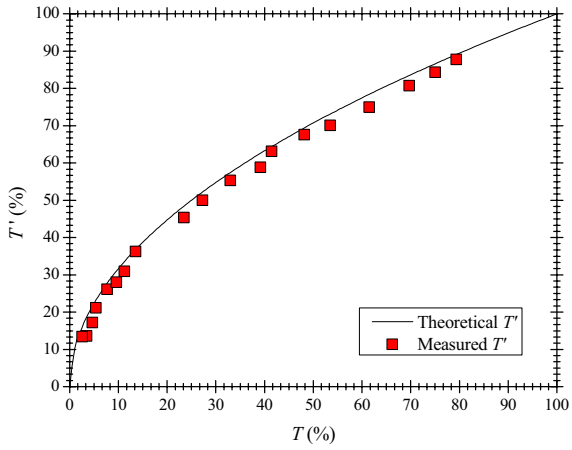

Fig. 5: Influence of the protecting tube (The theoretical *T'* is calculated from Eq. (2)).

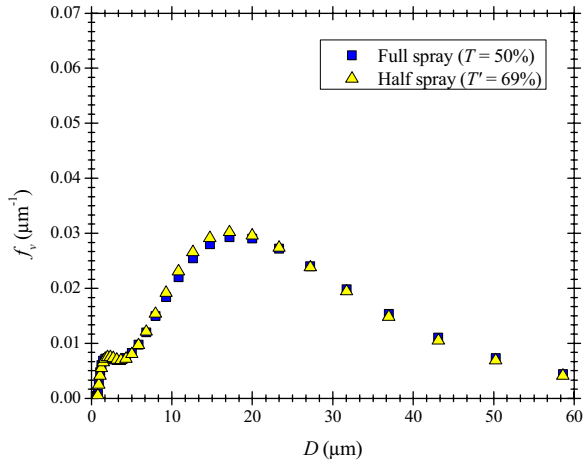

Fig. 6: Comparison of f_v with and without tube (ΔP_i = 5.47 MPa).

Finally, it was noted that measurements with the protecting tube couldn't remedy the beam steering effect. In

consequence, we decided to erase this undesirable effect by ignoring the signal collected by the six inner diodes in the drop-size distribution calculation.

2.3 Multiple Scattering Effects

Although many works showed that multiple scattering effects are not negligible for transmissions lower than 40%, it is necessary to check this limit because spray and experimental setup are not the same. To perform this, measured drop-size distributions with and without the tube are compared for injection pressures up to 13 MPa where the full spray measurement is still possible ($T > 5\%$).

Figure 7 (top) shows that drop-size distribution of half and full sprays are very close to each other and that there is no sign of multiple scattering. Therefore, in the present configuration, multiple scattering effects are found negligible for transmissions as low as 13%. The effects of multiple scattering appear when transmission is reduced to 11% as shown in Fig. 7 (bottom). Furthermore, this figure shows that the application of the correction patented by the Malvern Company doesn't report the expected distribution. Thus, the Malvern correction option is not adapted for the situation investigated in the present work.

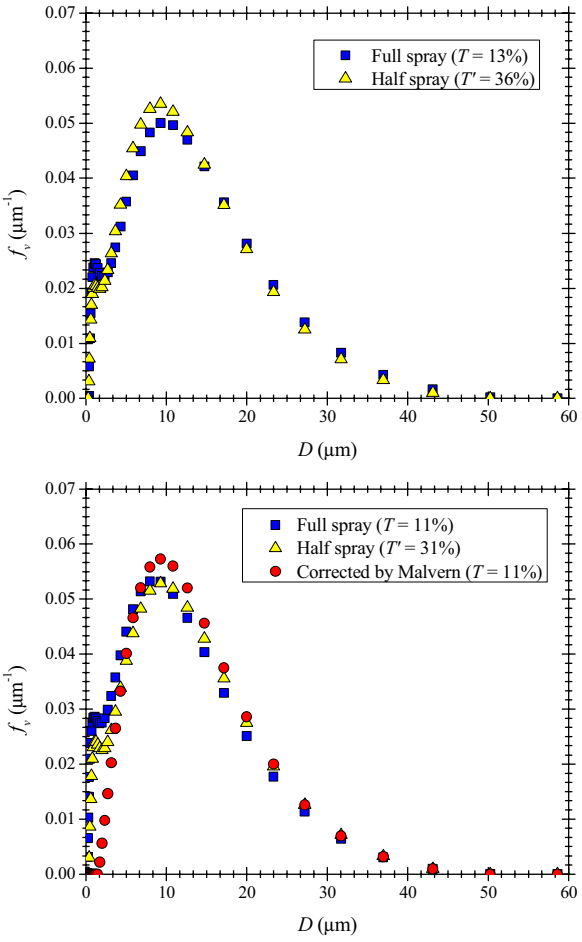

Fig. 7: Comparison of f_v with and without tube, (top) ΔP_i = 11 MPa, (bottom) ΔP_i = 11.5 MPa.

Figure 8 confirms that multiple scattering effects are effective when the full spray measurement transmission is less than 13%. This figure shows that the ratio of the measured (full spray) and actual (half spray) D_{43} reduces when transmission is less than 13%, while the ratio of measured and actual Δ_v increases. This result might be surprising but it is actually in agreement with previous observations. Indeed, considering low-injection pressure gasoline sprays, Triballier et al. [9] noticed that the transmission below which the mean diameter D_{43} decreased because of multiple scattering effects decreased as the injection pressure increases. Thus, multiple scattering effects appear at lower transmission when the spray is finer and the drop-size distribution narrower. The reduction of the transmission limit found here agrees with Triballier et al. [9] observations. We believe that this is due to the fact that, when the injection pressure increases, the drop-size distribution diameter range represents a lower and lower portion of the whole measurable diameter range, which is fixed by the collecting lens. However, in the present situation, correction of the multiple scattering effects must be performed when the transmission is lower than 13% corresponding to injection pressure greater than 11.5 MPa for the full spray.

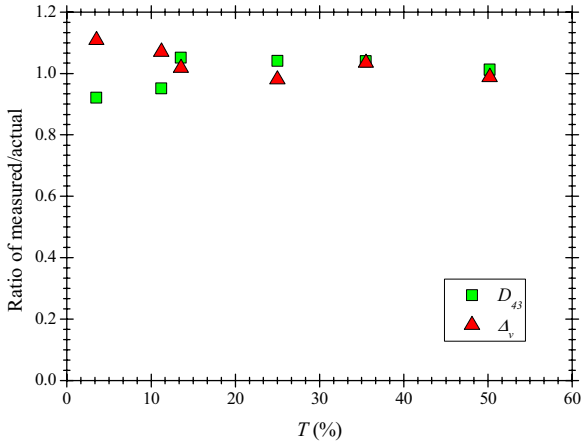

Fig. 8: Measured/actual of D_{43} and Δ_v.

The correction process is applied to scattered light intensity collected by diodes 7 to 35. The correction factor for each diode is assumed to be a function of transmission and is defined by:

$$\kappa_i(T) = \frac{I_i(T)}{I_i'(T')} \qquad i = 7, 8, \ldots, 35 \tag{3}$$

where I is the normalized measured scattered light intensity, I' the normalized actual intensity, and i the diode number. The actual intensity is the one obtained from half spray measurements provided that the injection pressure is less or equal to 15 MPa (see Fig. 4).

3 RESULTS AND DISCUSSION

3.1 Empirical Correction Factor

Figure 9 shows the measured correcting factors κ_i for several values of the transmission. As expected, when the transmission is high, κ_i is equal to 1 for each diode. At lower transmission, κ_i tends to increase for outer diodes and to decrease for inner diodes. These results indicate that the scattered light intensity at outer diodes must be reduced while the scattered light intensity at inner diodes must be increased. However, κ_i at the few outermost diodes (from 33 to 35)

shows the opposite trend: κ_i decreases and reaches value less than 1. This behavior illustrates the vignetting effects in full spray measurement. Therefore, κ_i for these diodes do not reflect only multiple scattering but also vignetting effects. As long as half spray measurement is not affected by vignetting; κ_i obtained for the outer diodes can be used to correct the vignetting effects.

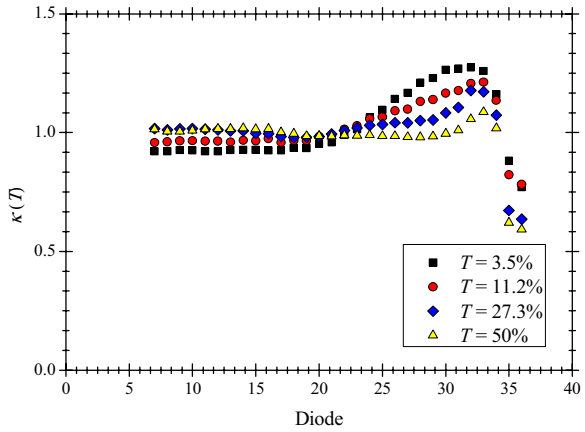

Fig. 9: Experimental correction factor κ_i for the diode series. Influence of the transmission.

Figure 10 shows the correction factors κ_i as a function of the transmission for several diodes. Based on these experimental data, the following mathematical function is suggested to derive analytical expression for the factors κ_i:

$$\kappa_i(T) = a_i - (a_i - \kappa_i(0))e^{\gamma_i T} \quad (4)$$

where a_i and γ_i are positive and negative parameters, respectively, and $\kappa_i(0)$ is the correction factor when the transmission is equal to zero. Normally, the constant a_i should be equal to 1 since κ_i becomes equal to 1 at high transmission. However, this is not the case for diodes 33 to 35 that are affected by vignetting effects as explained above. For these diodes, the parameter a_i is less than 1 as shown in Fig. 10. Thus, for each diode, two parameters have to be determined, namely, $\kappa_i(0)$ and γ_i. This is achieved by plotting the following expression for each diode:

$$ln(|a_i - \kappa_i(T)|) = ln(|a_i - \kappa_i(0)|) + \gamma_i T \quad (5)$$

When correction is not needed, γ_i and $\kappa_i(T)$ are taken equal to zero and a_i, respectively.

For each diode, Eq. (5) is plotted for full spray measurement transmission that indicates multiple scattering effects, i.e., $T < 13\%$. The result obtained for the 32nd diode is shown in Fig. 11 (top). Note that the mathematical expression given by Eq. (5) agrees well with the measurements. Thus, the values of the parameters γ_i and $\kappa_i(T)$ are determined from the linear regression. This procedure is reproduced for each diode to determine the analytical correction factor as a function of the transmission. Some of these analytical correction factors are shown in Fig. 11 (bottom). The results show that corrections for some median diodes are not needed whatever the transmission. The corrections for inner and outer diodes are important when transmission is less than 13%. Note that the correction factor of diode 35 has been shifted to 1 in order to use it on half spray measurements for which vignetting effects are negligible.

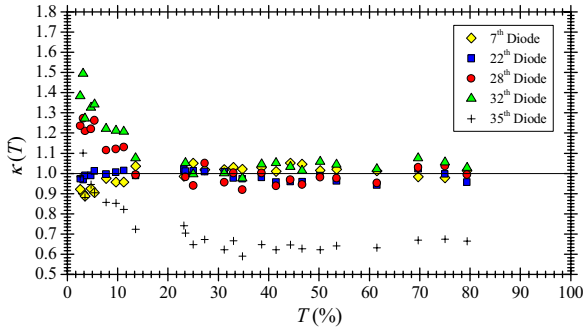

Fig. 10: Experimental evolution of κ_i with transmission for several diodes.

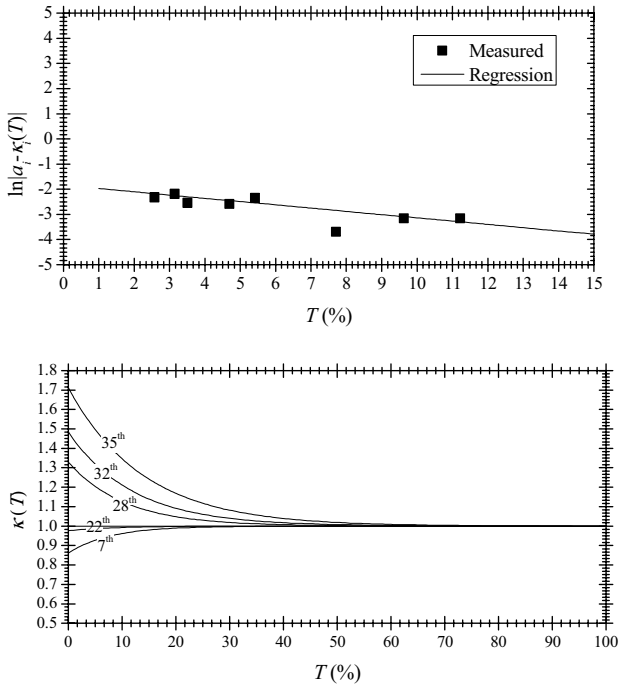

Fig. 11: (top) Eq. (5) plot for diode 32 (bottom) Analytical correction factors $\kappa_i(T)$ for several diodes.

3.2 Application of Correction Process and Results

The multiple scattering correction procedure using the analytical correction factors is tested on the full spray drop-size distribution that has a transmission $T = 3.5\%$ ($\Delta P_i = 14.5$ MPa). The corresponding distribution measured on the half spray is the actual spray drop-size distribution. The result is shown in Fig. 12 that presents both measured distributions as well as the one deduced from the correcting process. We see that the corrected drop-size distribution agrees very well with the actual drop-size distribution. Therefore, the correction process is used with confidence to derive the evolution of the spray drop-size distribution for injection pressure up to 20 MPa. For each injection pressure, the drop-size distribution we considered in this work was the one that reported the smallest mean diameter during the injection (see Fig. 3). Some of these distributions are presented in Fig. 13. This figure shows the increase of small drop production as the injection pressure increases. It can be

noticed also that the shape of the distribution evolves as a function of the injection pressure. For injection pressure less than 10 MPa, the distribution can be considered as mono-modal. However, for greater injection pressures, a peak in the small drop population develops and can't be ignored. We believed that the bi-modal drop-size distribution results from the specific liquid flow rearrangement during the atomization process. The liquid flow reorganizes as longitudinal ligaments. Visualizations (not presented here) revealed the presence of thin liquid lamella between the ligaments. The presence of these two flow structures could be at the origin of the production of two distinct drop populations.

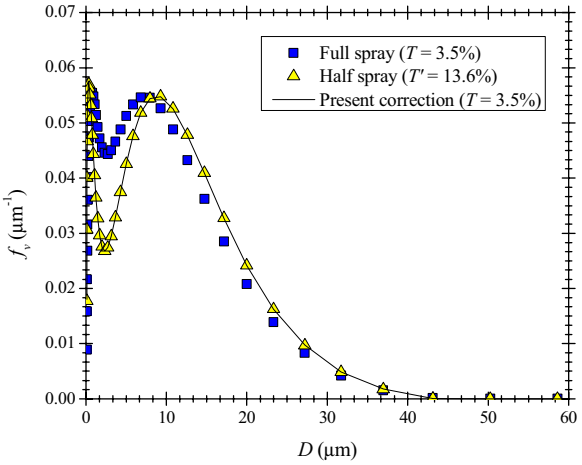

Fig. 12: Application of the multiple scattering correction process (ΔP_i = 14.5 MPa, T = 3.5%).

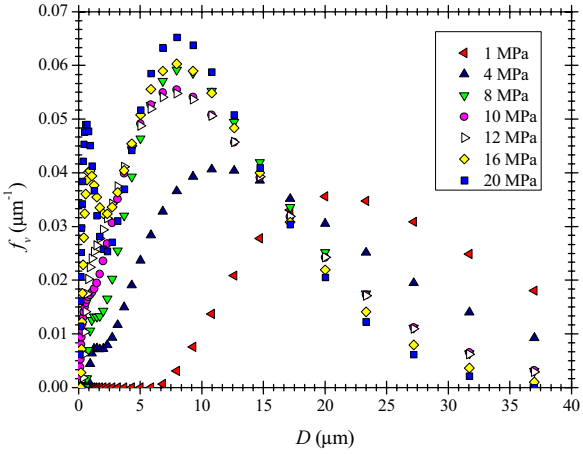

Fig. 13: Measured drop size distributions (T_i = 2 ms, z = 50 mm).

3.3 Drop-Size Distribution Modeling with MEF

In this section, the measured drop-size distributions are fitted with a mathematical function in order to derive a model to predict drop-size distribution for other injection pressures than those experimentally used. We suggest using the three-parameter Generalized-Gamma function that has been demonstrated to be the solution of the Maximum Entropy Formalism (MEF). (Details of the demonstration are available in [13].) The three-parameter Generalized-Gamma function is a single peak distribution. As shown in the previous section, the spray drop-size distributions for injection pressure greater than 10 MPa have two peaks. Thus, we suggest using a combination of three-parameter Generalized-Gamma functions, namely, the distributions are going to be fitted by a function of the form:

$$f_v(D) = (1-\beta) f_{v1}(D) + \beta f_{v2}(D) \tag{6}$$

where each component $f_{vi}(D)$ is given by:

$$f_{vi}(D) = \frac{q_i}{\Gamma\left(\frac{\alpha_i+3}{q_i}\right)} \left(\frac{\alpha_i}{q_i}\right)^{\frac{\alpha_i+3}{q_i}} \frac{D^{\alpha_i+2}}{D_{q_i0}^{\alpha_i+3}} exp\left(-\frac{\alpha_i}{q_i}\left(\frac{D}{D_{q_i0}}\right)^{q_i}\right) \tag{7}$$

where i = 1 or 2. In Eq. (6), $f_{v1}(D)$ and $f_{v2}(D)$ represent the small drop and the big drop population, respectively, and the parameter β, which may vary from 0 to 1, represents the volume fraction of the big drop population. Using the results commented in Fig. 13, when the injection pressure is less than 10 MPa, the drop-size distributions are assumed mono-modal. For this case Eq. (6) is simplified by setting $\beta = 1$. Thus, the number of parameters to be determined is a function of the injection pressure: when $\Delta P_i < 10$MPa, three parameters must be calculated, namely, q_2, α_2 and D_{q_20}, otherwise seven parameters must be determined, namely, q_1, α_1, D_{q_10}, q_2, α_2, D_{q_20} and β. In the first case ($\Delta P_i < 10$MPa) the three parameters are determined according to the methodology developed by Lecompte and Dumouchel [14]. This procedure (not detailed in the present paper) uses the Kullback-Leibler number, which quantifies the nearness between two distributions. This number is calculated for the mathematical function and the experimental distribution as a function of the parameters of the mathematical function. The best fit is obtained for the set of parameters that minimizes the Kullback-Leibler number. In the second case ($\Delta P_i \geq 10$MPa) this procedure is applied twice. First, it is applied on a portion of the experimental distribution limited by $D > D^*$ to determine the parameters q_2, α_2, D_{q_20} and β. Second, it is applied on the portion of the experimental distribution defined by $(f_v(D)-\beta f_{v2}(D))/(1-\beta)$ to determine the three remaining parameters, i.e., q_1, α_1 and D_{q_10}. In each situation, the diameter D^* is selected so that the $f_{v2}(D)$ function has the same peak diameter as the big drop population.

Lecompte and Dumouchel [14] emphasized that the parameters q and α must have the same sign but they can be either positive or negative. They noticed that the best sign for these parameters is, a priori, unknown. However, considering the results they reported, very fine sprays appeared to be best represented by negative parameters (see [14]). Thus, within the scope of this paper, q and α were assumed negative for both mathematical function components f_{v1} and f_{v2}.

Mathematical functions were determined as a function of the injection pressure. For each pressure, the drop-size distribution considered was the one that reported the smallest drop mean diameters. (Some of them are presented in Fig. 13.) Figure 14 presents two examples of fit, one for a low injection pressure (1 MPa, mono-modal distribution) and one for a high injection pressure (18 MPa, bi-modal distribution). It can be seen that in each case, the mathematical distribution offers a good representation of the measured distribution. Thus, the three-parameter Generalized Gamma function appears to be a very good candidate to represent the small-drop and the big-drop populations of the sprays.

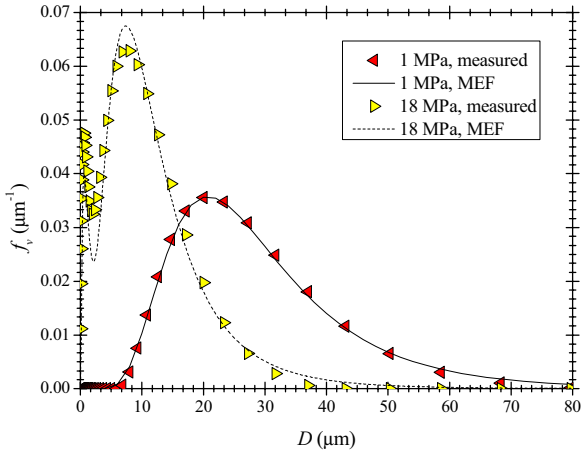

Fig. 14 Comparison between experimental and mathematical distributions.

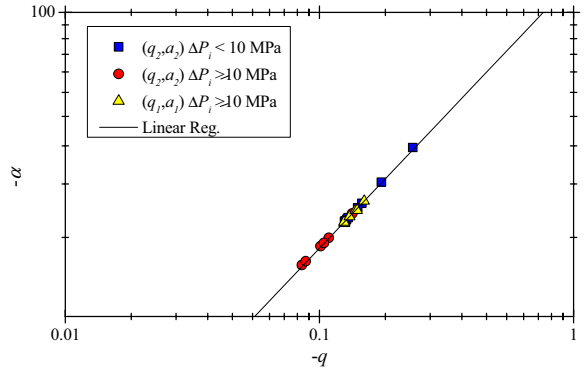

Fig. 15: Correlation between q_i and α_i.

Figure 15 shows, in a log-log scale, the correlation between the parameters q_i and α_i. The results for all injection pressures and for both mathematical distribution components are displayed. It can be seen that the two parameters correlate according to the relation:

$$|\alpha_i| = 127.2|q_i|^{0.88} \tag{8}$$

Lecompte and Dumouchel [15] demonstrated that the three-parameter Generalized-Gamma function is insensitive to a modification of the parameters q and α if they are related to each other according to a relationship similar to Eq. (8). In other words, if a series of spray drop-size distributions report parameters q and α satisfying such a relationship, these distributions have a constant shape and a unique couple (q; α) can represent the whole distribution series. In conclusion, a unique couple (q; α) can be used in the present work to characterize any distribution component. By calculating the average of the q-parameters and by deducing the corresponding α-parameter from Eq. (8), we found:

$$\begin{cases} q_i = -0.13 \\ \alpha_i = -21.5 \end{cases} \tag{9}$$

and this couple of values stands indifferently for i = 1 or 2.

Figure 16 shows the evolution of the other parameters as a function of the injection pressure. We note that each of them correlates well with the pressure and the following relationships can be derived according to the injection pressure:

$$\Delta P_i < 10 \text{ MPa} \qquad \begin{cases} D_{q_2 0} = 15.5 \Delta P_i^{-0.75} \\ \beta = 1 \end{cases} \tag{10}$$

and

$$\Delta P_i \geq 10 \text{ MPa} \qquad \begin{cases} D_{q_1 0} = 177 \Delta P_i^{-2.28} \\ D_{q_2 0} = 1.33 \Delta P_i^{0.39} \\ \beta = 1.29 \Delta P_i^{-0.12} \end{cases} \tag{11}$$

where the mean diameters are expressed in µm and the injection pressure in MPa. It could be surprising to obtain an increase of the mean diameter $D_{q_2 0}$ with the injection pressure as shown in Eq. (11). It must be kept in mind that this parameter characterizes a portion of the whole distribution only. As far as the whole distribution is concerned, this slight increase of $D_{q_2 0}$ with the injection pressure is compensated by a strong decrease of the corresponding $D_{q_1 0}$ and a decrease of the parameter β (see Eq. (11)).

It is concluded that the combination of Eqs. (6) and (7) offered a convincing approach to model the volume-based drop-size distribution produced by the high injection pressure gasoline injector studied in the present paper. Drop-size distributions can be predicted by associating Eqs. (9) and (10) or Eqs. (9) and (11) according to the injection pressure, paying attention that this parameter should be maintained lower or equal to 20 MPa.

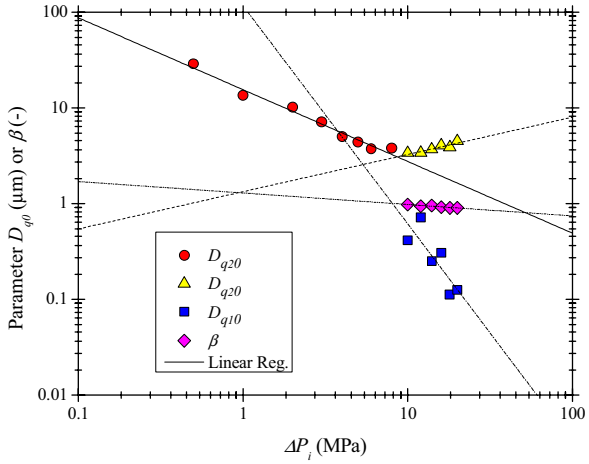

Fig. 16: Evolution of the mathematical distribution parameters with the injection pressure.

4 CONCLUSIONS

Spray drop-size distribution produced by a high injection pressure piezo injector has been successfully investigated by using a laser diffraction technique (Malvern Spraytec 2006). Because of the use of high injection pressures, a specific attention has been paid to the possible multiple scattering effects. Contrary to many previous works that found multiple scattering effects as soon as the transmission is lower than

40%, the present investigation reports a much smaller limit of the order of 13%. This result actually agrees with previous observations, which show that the limit in transmission decreases with the injection pressure. The small transmission limit found in the present work is believed to be due to specific characteristic features of the spray drop-size distributions. It was also found that the correction option of the Malvern is inappropriate to correct multiple scattering effects for transmission lower than 13%. In consequence, a specific procedure to correct these effects has been developed. This procedure is based on the determination of correction factors to be applied on the light intensity collected by each diode. These factors are functions of the transmission. Furthermore, analytical correction factors have been obtained in order to be able to provide a correction whatever the value of the transmission. It has been shown that the correction procedure using the analytical correction factors returned reliable drop-size distributions. Then, spray drop-size distributions can be obtained for injection pressure up to 20 MPa. It is found that the sprays produced by the piezo injector have a bi-modal drop-size distribution when the injection pressure is greater than 10 MPa. Such a spray characteristic is the consequence of the specific atomization mechanism that takes place on the flow issuing from the injector. Finally, the spray drop-size distribution has been successfully modeled by a MEF application, which returns mathematical distributions that are functions of 3 or 5 parameters according to the injection pressure. All these results will allow the temporal evolution of the spray drop-size distribution to be investigated and modeled during one injection event. This work is under consideration.

NOMENCLATURE

Symbol	Quantity	SI Unit
a_i	Parameter (Eq. (4))	-
D	Drop diameter	µm
D_{mn}	Mean diameter series	µm
f_v	Volume-based drop-size distribution	μm^{-1}
n	Refractive index	-
P_v	Vapor pressure	kPa
q, α	Parameters of Generalized-Gamma function	-
T, T'	Transmission	%
T_i , T_r	Injection time, time after injection	ms
ρ	Density	kg/m^3
ν	Kinematic viscosity	mm^2/s
σ	Surface tension	mN/m
τ	Spray turbidity	mm^{-1}
γ_i	Parameter (Eq. (4))	-
κ_i	Correction factor	-
ΔP_i	Injection pressure	MPa
Δ_v	Relative span factor	-
β	Volume fraction	-
Γ	Gamma function	-

REFERENCES

[1] W. F. Piock, S. Quelhas, G. M. Ramsay, J. Zizelman, and M. J. Frick, Gasoline Fuel Systems for Clean and Efficient Powertrains, *18 International AVL "Engine & Environment" conference*, pp. 1-13, Graz, 2006.

[2] H. Baecker, A. Kaufmann, and M. Tich, Experimental and Simulative Investigation on Stratification Potential of Spray-Guided GDI Combustion Systems, *SAE2007-01-1407*, 2007.

[3] G. Delay, B. Prosperi, R. Bazile, H. Nuglisch, and J. Hélie, FPIV Study of Gas Entrainment in a Hollow Cone Spray Submitted to Variable Density Using Fluorescent Particle Image Velocimetry, *Experiments in Fluids*, vol. 43, no. 2-3, pp. 315-327, 2007.

[4] L. G. Dodge, D. J. Rhodes, and R. D. Reitz, Drop-Size Measurement Techniques for Sprays: Comparison of Malvern Laser-Diffraction and Aerometrics Phase/Doppler. *Applied Optics*, vol. 26, pp. 2144-2154, 1987.

[5] S. Boyaval and C. Dumouchel, Deconvolution technique to determine local spray drop size distributions – Application to high-pressure swirl atomizers. *ILASS-Europe 2001*, Zurich Switzerland, 2001.

[6] P. Yongyingsakthavorn, P. Vallikul, B. Fungtammasan, and C. Dumouchel, Application of the Maximum Entropy Technique in Tomographic Reconstruction from Laser Diffraction Data to Determine Local Spray Drop Size Distribution, *Experiments in Fluids*, vol. 42, no. 3, pp. 471-481, 2007.

[7] L. G. Dodge, Change of Calibration of Laser Diffraction Based Particle Sizers in Dense Sprays. *Optical Engineering*, vol. 23, no. 5, pp. 626-630, 1984.

[8] T. Paloposki and A. Kankkunen, Multiple Scattering and Size Distribution Effects on the Performance of a Laser Diffraction Particle Sizer, *Proceeding of the International conference on Liquid Atomization and Spray Systems (ICLASS-91)*, Gaithersburg, MD, USA, pp. 441-448, 1991.

[9] K. Triballier, C. Dumouchel, and J. Cousin, A Technical Study on the Spraytec Performances: Influence of Multiple Scattering and Multi-Modal Drop-Size Distribution Measurements, *Experiments in Fluids*, vol. 35, pp. 347-356, 2003.

[10] T. L. Harvill and D. J. Holve, Method for Measuring Particle Size in the Presence of Multiple Scattering, United State Patent 5,619,324, 1997.

[11] O. L. Gulder, Multiple Scattering Effets in Dense Spray Sizing By Laser Difrraction, *Aerosol Science and Technology*, vol. 12, pp. 570-577, 1990.

[12] S. Boyaval and C. Dumouchel, Investigation on the Drop Size Distribution of Sprays Produced by a High-Pressure Swirl Injector: Measurements and Application of the Maximum Entropy Formalism, *Particle & Particle Systems Characterization*, vol. 18, pp. 33-49, 2001.

[13] C. Dumouchel, A New Formulation of the Maximum Entropy Formalism to Model Liquid Spray Drop-Size Distribution, *Part. Part. Syst. Charact.*, vol. 23, pp. 468-479 (2006)

[14] M. Lecompte and C. Dumouchel, On the Capability of the Generalized-Gamma Function to Represent Spray Drop-Size Distribution, *Part. Part. Syst. Charact.*, vol. 25, pp. 154-167 (2008)